Evaluation of plasma parameters on PEALD deposited TaCN

Fabien Piallat, Virginie Beugin, Remy Gassilloud, Philippe Michallon, Laurent Dussault, Bernard Pelissier, Timo Asikainen, Jan Willem Maes, François Martin, Pierre Morin, et al.

Evaluation of plasma parameters on PEALD deposited TaCN

Fabien Piallat[a,b,c,*], Virginie Beugin[b], Remy Gassilloud[b], Philippe Michallon[b], Laurent Dussault[c], Bernard Pelissier[c], Timo Asikainen[d], Jan Willem Maes[d], François Martin[b], Pierre Morin[a], Christophe Vallée[c]

[a]STMicroelectronics, 850 Rue Jean Monnet, 38920 Crolles, France
[b]CEA, LETI, Campus Minatec, 38054 Grenoble, France
[c]LTM-CNRS, 17 Rue Des Martyrs, 38054 Grenoble, France
[d]ASM Europe B.V. Versterkerstraat 8, 1322 AP Almere, The Netherlands

In this article influence of plasma parameters on TaCN deposition using Plasma Enhanced Atomic Layer Deposition (PEALD) is studied. TaCN is deposited on 300 mm Si substrate with the organometallic precursor Tertiary-ButylimidoTrisDiEthyl-aminoTantalum (TBTDET) and H_2/Ar plasma at different plasma power. Thickness, density, roughness, resistivity, crystallography and composition of the obtained layers were analysed by X-ray Reflection (XRR), 4 points probe measurement, X-ray Diffraction (XRD) and X-ray Photoelectron Spectrometry (XPS) respectively. Results show an evolution of the material with the increase of plasma power from a TaN-like to a TaC-like material.

1. Introduction

Sub-20 nm high-k/metal gate transistors, in replacement gate scheme, requires metal gate cavity filling with films as thin as 2 nm, with low resistivity, roughness and a good film conformity [1]. To fulfill these requirements the most used deposition method is the Atomic Layer Deposition (ALD) without or with plasma assistance (PEALD). Tantalum based alloys are know as chemical etch barrier and show chemical inertness as well as good thermal stability [2]. So TaCN electrode deposited by PEALD on HfO_2 dielectric is investigated as a possible candidate [3–6]. PEALD deposition method is based on alternation of metal–organic precursor decomposition with reactant gas and plasma steps for densification of the film. Tantalum metal–organic precursors currently available commercially are the PDEAT ($Ta(NEt_2)_5$) [7], PDMAT ($Ta(NMe_2)_5$) [8], TAIMATA ($Ta(NCMe_2Et)(NMe_2)_3$) [9] and TBTDET ($TaNCMe_3$)($NEt_2)_3$) [10], with Et and Me standing for ethyl and methyl groups, respectively. It was already proven that precursors are important not only because of their properties (vapour pressure, flash point and molecular weight mainly) but they also have an important influence on composition, electrical characteristics and oxidation of the deposited layer [11–13]. For this study commercial TBTDET was chosen due to low residue left after decomposition and its ability to be vaporised thanks to its low intrinsic vapour pressure (~1 Torr at 120 °C).

In this work, formation of tantalum carbo-nitride films deposited by ALD with H_2 plasma assistance, using different plasma conditions are presented and compared. Influences of plasma power on physical properties of the films are discussed.

2. Experimental methods

2.1. Samples preparation

All depositions were done in an ASM EmerALD®3000 chamber, on 300 mm silicon (1,1,1) substrate with a silicon thermal oxide of 100 nm for resistivity 4-points probe measurements. Tertiary-ButylimidoTrisDiEthyl-aminoTantalum (TBTDET) precursor was used for deposition. As presented Fig. 1b in the TBTDET molecule tantalum atom is bonded only with nitrogen, and one of the bounds is double, there is no direct bonding of tantalum and carbon.

Process steps of PEALD deposition are presented Fig. 1a. The process can be decompose as follow: introduction of precursor in the deposition chamber until surface saturation, purging excess of precursor, activating H_2/Ar plasma and purging before new surface saturation with precursor. Number of cycles is chosen depending on the targeted thickness, as the deposition rate is linear after the first cycles. In the current work, the number of cycles was fixed to

* Corresponding author at: CEA, LETI, Campus Minatec, F-38054 Grenoble, France.
E-mail address: fabien.piallat@cea.fr (F. Piallat).

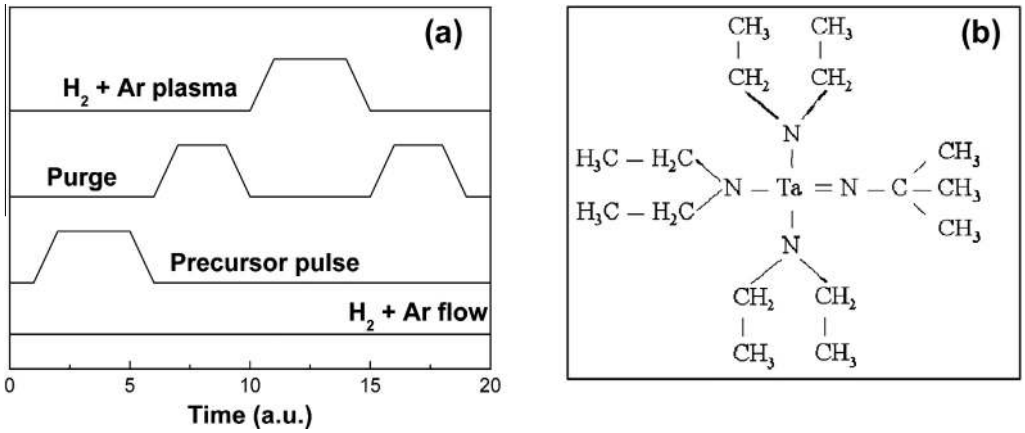

Fig. 1. (a) Plasma Enhanced Atomic Layer Deposition steps; (b) TBTDET molecule.

Table 1
Plasma time and plasma power used for each sample.

Time \ Power	LP	MP	HP
t_1	S1	S2	S3, S6
t_2		S5	
t_3	S4		

Constant plasma time
Constant plasma budget

320, which depending on plasma conditions lead to a film thickness ranging from 9 to 12 nm.

In this study, constant plasma time and constant plasma budget are compared. A first set of three films, S1, S2 and S3, was deposited at constant plasma time t_1 and variable plasma power: low power (LP), middle power (MP) and high power (HP). Three additional films, S4, S5 and S6, were processed at LP, MP and HP plasma power condition but with adapted plasma time t_3, t_2 and t_1 respectively, ($t_3 > t_2 > t_1$), in order to obtain a fixed product of plasma power by time, called plasma budget. These two sets of experiments allow a comparison of the influence of instant plasma power vs. total plasma budget on the TaCN film. The sample with the higher plasma power condition and a chosen plasma time t_1 was done twice (S3 and S6) in order to verify process repeatability. Used plasma powers and times are presented in the Table 1, with in line the constant plasma time and in diagonal the constant plasma budget.

2.2. Characterizations

Transfer from the deposition chamber to other characterization equipments required vacuum break, leading to surface oxidation of the films. To limit the variation of the oxide growth a minimum of one hour vacuum break was respected between deposition and characterization, in order to insure stabilisation of the oxide before analysis [14]. Thickness, density and roughness were measured by X-ray Reflection (XRR), in 43 points using a Jordan Valley JVX6200 (θ = [0; 3.5°]), and 4 points probe technique was used to measure the films resistivity in 49 points using Napson WS-3000. Crystallography of the samples was obtained by X-ray Diffraction (XRD) using a Panalytical X'Per Pro tool (θ = [30; 80°]) and compositions and chemical bonding were measured by X-ray Photoelectron Spectroscopy (XPS) using a Thermo Scientific Theta 300, with Al–Kα, 400 μm and 100 eV beam.

3. Results

3.1. Thickness and density

Fig. 2 shows XRR average thicknesses and densities versus plasma power, over the 43 measured points, extracted after careful spectra fitting. To obtain satisfying fit between the spectra and the model, 15 Å tantalum oxide layer was added on top of the TaCN layer, indicating a clear surface oxidation of the film.

Besides, layer roughness did not change with plasma modification, thus results are not discussed in the current paper.

It appears that the two samples S3 and S6 generated at HP present a similar variation of thickness and density included in the measurement error margin. This similarity was confirmed with resistivity measurements. Thus process is considered as stable.

First, for constant plasma time experiments, thickness decrease (left axis) and density increase (right axis) are observed at higher plasma power, which indicates a densification of the material (see (2) on Fig. 2). Measured density, 10.5 g cm^{-3} for LP and 11.5 g cm^{-3} for HP, has to be compared with theoretical density of TaN: 13.7 g cm^{-3} and TaC: 14.5 g cm^{-3} [15]. Difference between theoretical and experimental density values could be related to TaCN surface oxidation.

Second, for the constant plasma budget experiments, a decrease of thickness and increase of density with longer plasma time at both LP and HP conditions are observed. At constant plasma budget a significant variation of density and thickness can be observed between S4 LP and S6 HP (see (1) on Fig. 2). Therefore comparing the two sets of experiments it appears that plasma time increase is leading to lower changes in the material than plasma power increase. Higher plasma power seems to be necessary to break down the precursor molecule and enable creation of new bonds.

Resistivity of the layers, Fig. 2, exhibits similar behaviour as the thickness presented previously.

Constant plasma time experiment shows a decrease of resistivity with a factor 8 from LP to HP samples. From literature it is known that cubic-TaN (150 μΩcm) is more resistive than cubic-TaC (30 μΩcm) [15] for highly crystalline samples. Therefore, it shows that plasma power increase changes the materials properties from TaN-like to TaC-like film. Obtained resistivity is comparable with resistivity of films deposited by MOCVD [16] and reactive sputtering [17,18] techniques, as it is ranging from 200 to 1000 μΩcm depending on process conditions.

In line with the previous XRR study, it appears that LP and HP samples in the constant plasma budget experiment show a decrease of resistivity. Effect of plasma time increase on resistivity is obvious (see Fig. 2 S1, S4 at LP and S2, S5 at MP) but not as efficient as a plasma power increase (HP values). Here again, one can conclude that higher plasma power is more efficient to decompose the precursor than longer plasma time.

In the rest of the discussions, focus will be done on constant plasma time experiments, S1, S2 and S3 samples, which represent extreme cases (i.e. the other samples are expected to present intermediate properties).

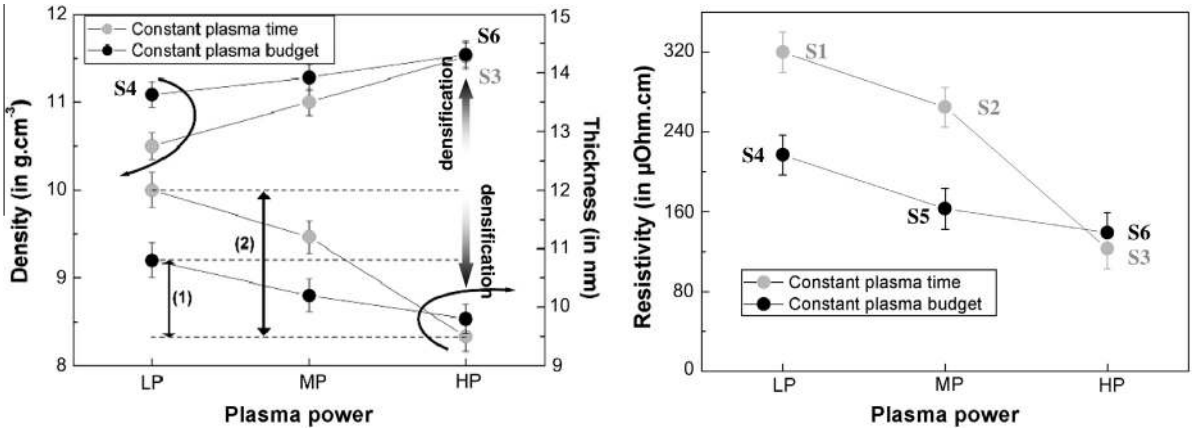

Fig. 2. Evolution of thickness, density (left) and resistivity (right) depending on plasma parameters.

3.2. Crystallography

Crystallographic spectra of LP and HP samples are presented in Fig. 3, along with the theoretic peaks of cubic-TaN and cubic-TaC. Spectrum from MP sample is not displayed to allow a better view of LP and HP differences.

Five Miller indexes are visible in the analysed window, these indexes confirm that both LP and HP samples have a cubic structure. Moreover, matching between experimental spectra and theoretical peaks shows that the increase of plasma power is changing the crystallography of the films from cubic-TaN to cubic-TaC, this evolution is clearly visible for all the indexes.

The shift of the crystallographic peaks is related to a modification of the lattice parameter of the layer, from 4.32 Å at LP to 4.42 Å at HP. These two values perfectly match with reported cubic-TaN and cubic-TaC lattice parameter [19].

In addition, the artefact from substrate silicon (1, 1, 1) at $\theta = 57°$, visible for both LP and HP samples, shows that the shift in peaks location is not due to measurement error but corresponds to a change in the deposited material.

Although, spectrum of the intermediate power sample (MP) is not presented here, we notice that the five indexes peaks are all located in between LP and HP peaks. Full width at half maximum (FWHM) and intensity of the peaks are similar for the three samples, which shows that it exists only one kind of lattice within the layer. If MP layer would be made from a mixture of TaN and TaC polycrystals an enlargement of the peaks together with a decrease of intensity would have been observed. Thus modification of lattice size is gradual with plasma power increase.

The high intensity and low FWHM of the peaks in the spectra means that the material is highly crystalline. So the lower density observed in the Section 3.1 cannot be explained by a low crystallinity of the layer.

3.3. Chemical environments

The chemical environment of the species in LP and HP layers was deduced from XPS analysis. Ta4f, C1s and N1s spectra acquired on LP samples are presented in Fig. 4, HP sample Ta4f, C1s and N1s are presented in Fig. 5.

Ta4f spectra from LP sample, Fig. 4, and HP sample, Fig. 5, exhibit three environments; Ta–O (i.e. Ta bonded with oxygen), Ta–N and Ta–C located at 26, 24.5 and 23.5 eV, respectively [20]. Because of the three overlaid bonding environments, analysis of the spectra is quite difficult. In order to have more information on the material bonding, environments of carbon and nitrogen were studied, with C1s and N1s respectively. Spectra are presented Fig. 4 for LP sample and Fig. 5 for HP sample. Environment changes of C1s and N1s are clearly highlighted on these spectra. On Figs. 4 and 5 C1s peaks present at 283 eV (on the right of the spectra) correspond to C-Ta bonds. Figs. 4 and 5 N1s peaks present at 397 eV (on the right of the spectra) correspond to N–Ta bonds. Evolution of carbon and nitrogen bonds is consistent with the hypothesis expressed above: plasma power increase allows a better precursor's molecule bonds separation which changes the material from TaN-like to TaC-like.

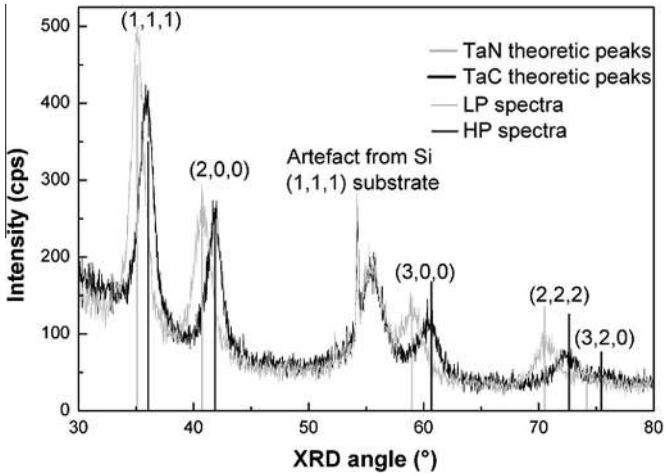

Fig. 3. XRD analysis S1 and S3 TaCN layers along with cubic TaN and cubic TaC theoretical peaks.

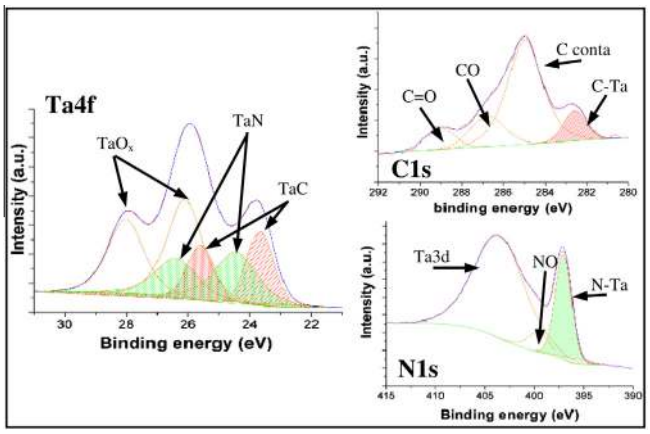

Fig. 4. XPS spectra of Ta4f (a), C1s (b) and N1s (c) for LP sample.

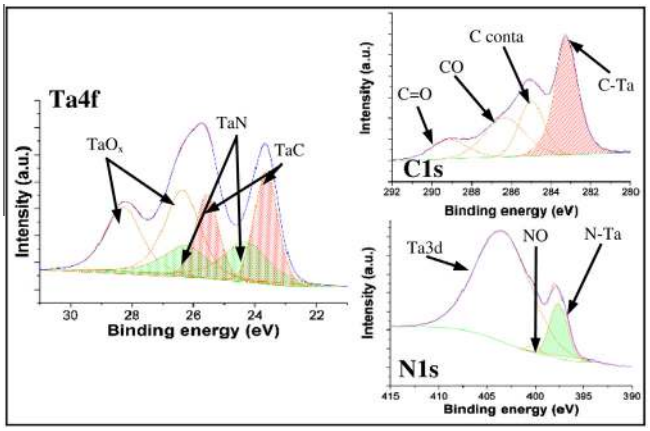

Fig. 5. XPS spectra of Ta4f (a), C1s (b) and N1s (c) for HP sample.

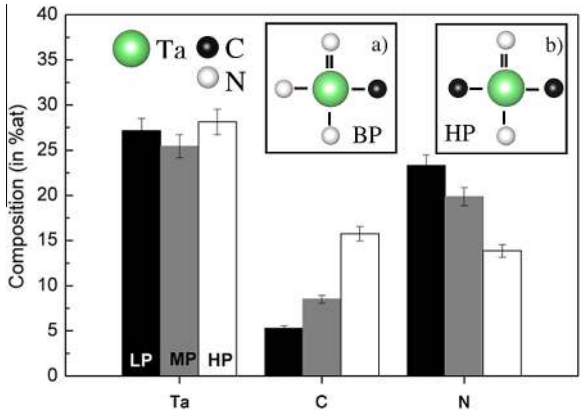

Fig. 6. Samples composition at constant plasma time and representation of bonding for LP (a) and HP (b) samples.

Quantification of the species present in the films can be extracted from the current XPS spectra, leading to the composition of the layers. Indeed, area under the curve is proportional to the number of bonds present in the analysed volume. Films compositions are given in Fig. 6. This estimation only includes C–Ta (obtained in C1s), N–Ta (obtained in N1s) and Ta–C, Ta–N bonds (obtained in Ta4f).

Layers compositions reveal that the number of carbons in C–Ta bonds is increasing with higher plasma power, whereas nitrogen in N–Ta bonds is decreasing. This observation further confirms modification of the material from TaN-like to TaC-like, keeping a TaC_xN_{1-x} composition.

Representation of Ta atoms and their bonds for LP and HP are given Fig. 6a and b, it reflects the composition changes of the deposited layers from $TaC_{0.19}N_{0.86}$ at LP to $TaC_{0.56}N_{0.49}$ at HP.

4. Discussion

4.1. Film composition

Overall, characterizations done in this study proved the evolution of TaCN metal properties from TaN-like to TaC-like material. This evolution was linked to the increase of plasma power which allows to break chemical bond between Ta and N in the TBTDET molecule, resulting in an increase of tantalum bonded with carbon in the deposited material. Also due to the original chemical structure of TBTDET molecule, nitrogen concentration in the layers is greater than carbon concentration. Complete replacement of nitrogen by carbon has not been seen, even with higher plasma power than presented here. This observation can be associated to the presence of a double bond between Ta and N, plasma energy necessary to break this bond is more important.

On the XPS spectra presented Section 3.3 no C–N, N–N nor Ta–Ta bonds were observed, whatever the plasma parameters. Therefore it appears that all C and N coming from the precursor molecule either react with Ta to form Ta–C or Ta–N bonds or is pumped away from the sample surface as a deposition by-product. No residues, such as $N(CH_3)_3$ or CH_4 are detected in the film. The absence of carbon impurities in the film and the presence of Ta–C explain the low resistivity of the layers, indeed carbon impurities increase the resistivity of the films [21], whereas carbides decrease it.

4.2. Film density

Crystallographic analysis of the samples, Section 3.2, showed a high cristallinity of the films, suggesting that experimental density should be similar to theoretical one. Using Angle Resolved XPS, the surface oxidation was determined to be thinner than 2 nm. Knowing that Ta_2O_5 density is 8.2 $g\,cm^{-3}$ [15], a stack of 2 nm of Ta_2O_5 and 10 nm of TaN or TaC has an total density of 12.5 or 13.3 $g\,cm^{-3}$ respectively. Thus surface oxide may not be the only cause of the lower density. Another hypothesis to explain the density shift is the oxidation of the first deposited nanometres by interaction with the substrate. It has been shown that ALD deposited TaN is creating only Ta–O bonds in the early steps of the process [22]. Thus it can be supposed that there is oxidation of TaCN, located at the TaCN/SiO_2 interface, but because of TaCN surface oxidation it is not possible to locate the Ta–O bond with the available tools. A 1 nm tantalum oxide at the substrate interface would decrease the density from 12.5 to 11.9 and 13.3 to 12.7 $g\,cm^{-3}$ for TaN and TaC respectively. On top of that the XRR fitting error has to be taken into consideration. This error which can be evaluated to 10%, leading to a measured density of TaN or TaC matching to the theoretical densities of crystalline material.

4.3. Film formation

TBTDET metalorganic precursor has similar behaviour to other metalorganic precursors, such as TDMAT, as metal is only bonded to nitrogen. Thus deposition of TBTDET can be resolved by three different reactions [23]: transamination exchange with the formation of trimethylamine and methane (1), amine elimination (2) and (3) and possible transposition reaction creating ammonia and hydrogen (4) or nitrogen and hydrogen (5).

Formula (1): precursor TBTDET deposition at sample surface under H_2 flow.

$$Ta[N(CH_2CH_3)_2]_3[=NC(CH_3)_3] + 6H_2(g) \rightarrow N_2Ta[N(CH_2CH_3)_2][=NC(CH_3)_3] + 8CH_4 \quad (1)$$

Formula (2) and (3): amine elimination forming Ta–H (2) or Ta–N (3).

$$N_2Ta[N(CH_2CH_3)_2][=NC(CH_3)_3] + H_2plasma \rightarrow N_2TaH_2 + 2N(CH_3)_3 + 2CH_4 \quad (2)$$

$$N_2Ta[N(CH_2CH_3)_2][=NC(CH_3)_3] + H_2plasma \rightarrow N_2Ta(NH_2)_2 + 8CH_4 \quad (3)$$

Formula (4) and (5): possible transposition reactions of N by C to form TaC from TaN

$$TaN + CH_4(g) \rightarrow TaC + NH_3(g) + 1/2H_2 \quad (4)$$

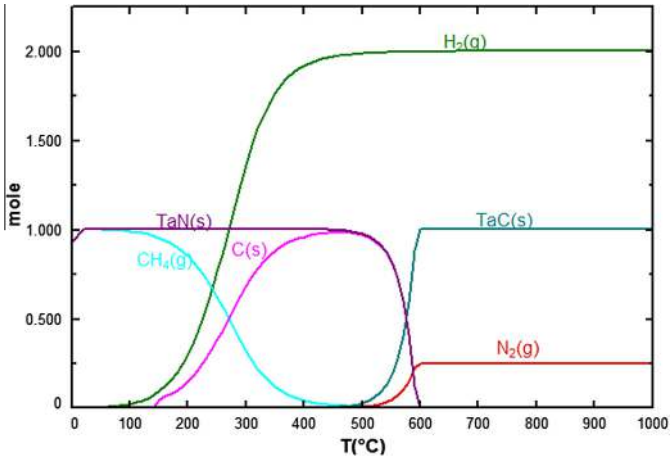

Fig. 7. Evolution of the Gibbs energy of the products from the reaction (2).

$$TaN + CH_4(g) \rightarrow TaC + 1/2N_2(g) + 2H_2 \quad (5)$$

To explain the creation of TaC with plasma power increase the Gibbs energy of the transposition reaction was calculated. Considering that in this experiment deposition is done at 325 °C and under 1 Torr the Gibbs energy of reaction (5) can be determined to be +77 kJ/mol, thus the reaction is not spontaneous. But a temperature increase will lead to the enhancement of TaC creation, as shown in Fig. 7. Calculation reports that transposition reactions (4) and (5) appear from 550 °C, such temperature can be reached locally at the sample surface thanks to hydrogen plasma. As a result increase of H_2 plasma power is leading to an increase of the local temperature and will promote the transposition reaction, leading to creation of TaC.

XRD measurements, Section 3.2, showed a gradual change of the lattice parameter from cubic-TaN to cubic-TaC but composition analysis, Section 3.3, proved that the material always contains nitrogen and carbon. Thus it appears that increase of plasma power is leading to introduction of carbon atoms in TaN lattice, progressively affecting the lattice parameter of the material toward a TaC lattice. One can suppose that this carbon nitrogen exchange and evolution of the lattice parameter is leading to high internal stress of the material, a study of this stress is ongoing.

5. Conclusion

In this study the influence of plasma power on TaCN films deposited by PEALD was evaluated. XRR and four points probe measurements showed that using higher plasma power: lower resistivity and higher density films were obtained. These changes were compared with theoretical data of TaN and TaC material to highlight the similarities and it appeared that increase of plasma power is shifting the material from a TaN-like to a TaC-like material. Increasing plasma time to have same plasma budget at all plasma power (product of plasma power and plasma time constant) led to a decrease of the observed variations between low and high plasma power, but differences are still significant. XRD analyses support the TaN-like and TaC-like hypothesis with really good fitting of the experimental and theoretical Miller indexes. Then, a correlation was done with XPS measurement, proving the hypotheses of TaN-like and TaC-like materials thanks to chemical bonding and film composition. XPS analysis also showed a significant O contamination due to post-oxidation of TaCN films in ambient atmosphere. Finally, a reaction mechanism was proposed to explain the creation of TaC from the TaN bond initially present in the TBTDET molecule.

Acknowledgements

This work was achieved with the help of the LETI DTSI silicon platform and ST Crolles 2 300 mm fabline in the frame of ST/LETI joined development program.

References

[1] P. Packan et al., IEDM Tech. Dig. (2009) 659.
[2] H. Zhu, R. Ramprasad, J. Appl. Phy. 109 (2011) 083719.
[3] J.S. Park, M.J. Lee, C.S. Lee, S.W. Kang, Electrochem. Solid-State Lett. 4 (2001) C17.
[4] J.S. Park, H.S. Park, S.W. Kang, J. Electrochem. Soc. 149 (2002) C28.
[5] C.S. Lai, W.C. Wu, J.C. Wang, T.S. Chao, Appl. Phys. Lett. 86 (2005) 222905.
[6] Y. Sugimoto et al., Thin Solid Films 517 (2008).
[7] S.L. Cho, K.B. Kim, S.H. Min, H.K. Shin, S.D. Kim, J. Electroc. Soc. 146 (1999) 3724–3730.
[8] E.R. Engbrecht, Y.M. Sun, S. Smith, K. Pfiefer, J. Bennett, J.M. White, et al., Thin Solid Films 418 (2002) 145.
[9] J.W. Hong et al., in: Proceedings of the IEEE International Interconnect Technology Conference, 2004.
[10] H.T. Chiu, S.H. Chuang, C.E. Tsai, G.H. Lee, S.M. Peng, Polyhedron 17 (1998) 2197.
[11] H. Matsuhashi, C.-H. Lee, T. Nishimura, K. Masu, K. Tsubouchi, Mat. Sci. In Semicond. Proc. 2 (1999) 303.
[12] J.G. Lee et al., in: Proceedings of the 1996 MRS Spring, Symposium, 1996.
[13] H. Wojcik et al., in: Proceedings of the IEEE International Interconnect Technology Conference, 2007.
[14] P.B. Sewell, D.F. Mitchell, M. Coehn, Surf Sci. 29 (1972) 173–188.
[15] Material Property Data. Available at: www.matweb.com, 2012.
[16] M.H. Tsai, S.C. Sun, H.T. Chiu, C.E. Tsai, S.H. Chaung, Appl. Phys. Lett. 67 (1995) 1128.
[17] M.A. Farooq, S.P. Murarka, C.C. Chang, F.A. Baiocchi, J. Appl. Phys. 65 (1989) 3017.
[18] B. Mehrota, J. Stimmell, *J. Vac. Sci. Technol.* B 5 (1987) 1736.
[19] National Institute of Standards and Technology, NIST XRD, Database, 2012.
[20] J.-F. Moulder et al., Handbook of X-Ray Photoelectron Spectroscopy, Perkin-Elmer Corporation, 1992.
[21] K.-E. Elers et al., J. Electrochem. Soc. 152 (2005) G589.
[22] F. Volpi et al., Microelectron. Eng. 85 (2008) 2068.
[23] P. Caubet et al., J. Electrochem. Soc. 155 (2008) 8.